AD-A052 554 NAVAL RESEARCH LAB WASHINGTON D C F/G 20/7
COMPUTER SIMULATION OF SPACE CHARGE EFFECTS IN PARTICLE ACCELER--ETC(U)
JAN 78 I HABER

UNCLASSIFIED NRL-MR-3705 SBIE-AD-E000 131 NL

| OF |
AD
A052 554

END
DATE
FILMED
5-78
DDC

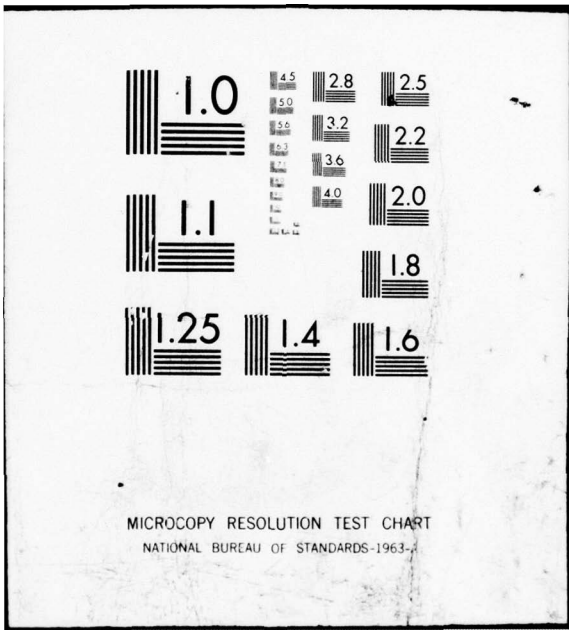
1.0
1.1
1.25
1.4
1.6
1.8
2.0
2.2
2.5
2.8
3.2
3.6
4.0
4.5
5.0
5.6
6.3
MICROCOPY RESOLUTION TEST CHART
NATIONAL BUREAU OF STANDARDS-1963-A

15 MAR 78

ADE000131

NRL Memorandum Report 3705
Interim rept.

Computer Simulation of Space Charge Effects in Particle Accelerators.

IRVING HABER
Plasma Dynamics Branch
Plasma Physics Division

NRL-MR-3705

Jan[redacted]78

32 p.

SBIE

AD-E000 131

NAVAL RESEARCH LABORATORY
Washington, D.C.

251 950

SECURITY CLASSIFICATION OF THIS PAGE (When Data Entered)

REPORT DOCUMENTATION PAGE		READ INSTRUCTIONS BEFORE COMPLETING FORM
1. REPORT NUMBER NRL Memorandum Report 3705	2. GOVT ACCESSION NO.	3. RECIPIENT'S CATALOG NUMBER
4. TITLE (and Subtitle) COMPUTER SIMULATION OF SPACE CHARGE EFFECTS IN PARTICLE ACCELERATORS		5. TYPE OF REPORT & PERIOD COVERED Interim report on a continuing NRL problem. 6. PERFORMING ORG. REPORT NUMBER
7. AUTHOR(s) I. Haber		8. CONTRACT OR GRANT NUMBER(s)
9. PERFORMING ORGANIZATION NAME AND ADDRESS Naval Research Laboratory Washington, D.C. 20375		10. PROGRAM ELEMENT, PROJECT, TASK AREA & WORK UNIT NUMBERS NRL Problem No. H02-58
11. CONTROLLING OFFICE NAME AND ADDRESS Department of Energy Washington, D.C. 20345		12. REPORT DATE January 1978 13. NUMBER OF PAGES 32
14. MONITORING AGENCY NAME & ADDRESS(if different from Controlling Office)		15. SECURITY CLASS. (of this report) UNCLASSIFIED 15a. DECLASSIFICATION/DOWNGRADING SCHEDULE

16. DISTRIBUTION STATEMENT (of this Report)

Approved for public release; distribution unlimited.

17. DISTRIBUTION STATEMENT (of the abstract entered in Block 20, if different from Report)

18. SUPPLEMENTARY NOTES

This research was sponsored by the U.S. Department of Energy.

19. KEY WORDS (Continue on reverse side if necessary and identify by block number)

Inertial confinement fusion
Heavy ion fusion
Accelerator technology
Beam transport

20. ABSTRACT (Continue on reverse side if necessary and identify by block number)

The potential use of high energy ion beams as a source of thermonuclear pellet ignition energy has increased the importance of understanding high current beam transport. Computer simulation using particle codes promises to be a useful tool in gaining that understanding. A series of simulations is presented in which the numerical parameters are systematically varied to illustrate the purely numerical effects on these simulations in a physically interesting parameter range. It is found that the significant effects observed are essentially independent of the numerical

→ Next Page

(Continues)

DD FORM 1 JAN 73 1473 EDITION OF 1 NOV 65 IS OBSOLETE
S/N 0102-014-6601

SECURITY CLASSIFICATION OF THIS PAGE (When Data Entered)

20. Abstract (Continued)

parameters. It therefore appears that the numerical techniques are indeed capable of reliably predicting the behavior of actual beam transport systems.

CONTENTS

COMPUTER SIMULATION OF SPACE CHARGE EFFECTS IN PARTICLE ACCELERATORS

I. Introduction

Recent studies[1] have indicated the feasibility of using intense energetic heavy ion beams as the source of ignition energy for inertially confined nuclear fusion reactions. It appears that heavy ion beams with suitable powers and energies can be produced using modest extrapolations of conventional particle accelerator technology. However, one of the major limits on the beam intensities which can be delivered to a target is due to the space charge repulsive forces of the beam particles themselves. It has therefore become important to examine the effects of these space charge forces on particle focussing and transport.

The transport of charged particle beams is well understood when the space charge densities are small.[2] In this limit, the particle trajectories can be accurately described by their single particle orbits in the external focussing fields. A commonly employed focussing system uses alternate gradient quadrupole magnets. We will assume that all particles have the same longitudinal velocity and proceed to discuss the transverse behavior of quadrupole systems.

If the plane perpendicular to the direction of beam propagation is described in rectangular coordinates properly aligned with respect to the quadrupole magnet pole tips, each particle is subjected to an

Note: Manuscript submitted January 16, 1978.

x-directed force proportional to its x distance from the center of the system and a y-directed force proportional to its y distance from the center. If this force is focussing in x, it is defocussing in y. Each successive magnet is then rotated 90^{o} so that in each direction a particle is alternatively focussed and defocussed. However, the net effect is focussing in both directions.

A particle which starts off center, is focussed towards the center, goes past it, and eventually returns through its initial position, thereby executing a periodic motion. The fraction of this period excecuted per lens pair, is a phase shift μ_o given by[2]

$$\text{Cos } \mu_o = 1 - \eta^2/2 \qquad (1)$$

where $\eta = v_z\tau/F$, $v_z\tau$ is the distance between succeeding lenses. 2τ is therefore the time taken to traverse a complete lens doublet.

If the trajectory of a particle in $x\text{-}p_x$ phase space is plotted as it passes through successive focussing lenses, in the non-degenerate case where $\mu_o \neq \frac{n\pi}{m}$, the particle traces an ellipse. Every other particle which has an initial phase space location on this same ellipse also remains on it, so that an initial phase space distribution which is uniform along this ellipse remains that way. A beam which fills such an ellipse will retain a constant cross section as it passes through succeeding lens systems and is spoken of as a matched beam. The product $x_o p_{xo}$, which is the area of the ellipse in phase space divided by π, is known as the emittance ε.

Fig. 1a shows the $x\text{-}p_x$ phase space of such a matched ellipse of particles half way through a focussing lens. Fig. 1b shows the phase space 2/5 way to the next (defocussing) lens. Fig. 1c shows the phase space half way through the defocussing lens. Fig. 1d shows the phase space of the ellipse now having executed 4/5 of its period and Fig. 1e shows the ellipse back where it started. It should be noted that though the ellipse looks as it did when it started, the individual particles have moved only μ_o degrees (in this case $\mu_o = 90^o$) around the ellipse. The space charge forces in this case are negligibly small.

In the presence of space charge forces, the beam transport system becomes somewhat more complex. Each particle orbit is no longer independent of the others and the x and y directions are no longer decoupled. However, by assuming a particle distribution function of the form

$$f(r,p) = \delta \left[(x/x_o)^2 + (y/y_o)^2 + (p_x/p_{xo})^2 + (p_y/p_{yo})^2 - r_o^2 \right], \quad (2)$$

which is uniformly distributed on the $x\text{-}p_x\text{-}y\text{-}p_y$ hyper-ellipse, Kapchinskij and Vladimirskij[3] (K-V), have derived a self-consistent set of equilibria for focussing systems in the presence of space charge. By assuming such an idealized K-V distribution function, the beam dynamics including space charge can be described by a pair of coupled ordinary differential equations for the two configuration space axes of the K-V hyper-ellipse. These may be written in the form of Lambertson, Laslett and Smith[4] as

$$\frac{d^2u_x}{d\theta^2} = -S_x(\theta)u_x + \frac{1}{u_x^3} + \frac{Q}{u_x+u_y},$$

$$\frac{d^2u_y}{d\theta^2} = -S_y(\theta)u_y + \frac{1}{u_y^3} + \frac{Q}{u_x+u_y} \tag{3}$$

where θ is a normalized distance along the beam, u_x and u_y are proportional to the major axes of the elliptical beam cross sections in x and y. The focussing term $S(\theta)$ is a unit amplitude δ function in the thin lens approximation. The dimensionless parameter

$$Q = \frac{4q^2}{A}\frac{Nr_p}{\beta\gamma^2\varepsilon K^{1/2}} \tag{4}$$

where r_p is the classical proton radius and K=1/fL is the lens strength, is a measure of the strength of the space charge effects on the beam. Since the space charge forces are repulsive and therefore act against the lens focussing forces, the phase shift per lens system, μ, is less than the value μ_o in the absence of space charge. Since it is a property of the K-V distribution that the space charge forces are linear, μ is the same for all beam particles and can also serve as a measure of the amount of space charge. It is significant to note that in the absence of space charge there is only one free parameter. That is, the distance between lenses, which is related to the phase shift per cell μ_o. Adding the space charge then, the system of equations has two free parameters. These beam envelope equations can be integrated numerically to obtain the behavior of this special class of space charge systems.[4,5]

The analysis of space charge effects by integrating the equations for the axes of a K-V distribution suffers from a number of fundamental limitations. Only uniformly loaded ellipses of the K-V form are treated. Therefore, any collective behavior not characteristic of a uniformly loaded ellipse can not be represented. Degrees of freedom expected to occur in a real system such as deviation from either uniformity or ellipticity can not be represented. Therefore, even if the K-V distribution were a realistic initial distribution, the stability of this system to realistic perturbations can not be investigated within the K-V formalism. Many physical effects which can be of crucial importance to successful accelerator design may be missed by this approach.

II. The Numerical Model

Standard particle simulation techniques[6] can be employed to investigate finite space charge beam transport somewhat more generally than is possible by following the K-V envelope equations. Since the beam is long compared with its transverse dimensions, non-uniformities of the beam in the direction of propagation are neglected. By working in a reference frame moving with the beam, the evolution of the beam as it propagates in the z direction translates into the temporal evolution as viewed in the x-y plane. In this reference frame the magnet forces become electrostatic forces.

The numerical time differencing is shown in Fig. 2. The particle velocities and positions are defined one half time step apart. The particle positions are advanced according to

$$x_{t+\Delta t} = x_t + v_{t+\Delta t/2}\,\Delta t. \tag{5}$$

The particles at the new times are then accumulated onto a grid to give a charge density array. Poisson's equation is then solved using fast Fourrier transforms to give the electric fields self-consistent with the charge density. These electric fields are then used to change the velocities according to

$$v_{t+3\Delta t/2} = v_{t+\Delta t/2} + (q/m)E_{t+\Delta t}\Delta t \tag{6}$$

This numerical algorithm is time centered, reversible and second order accurate. It is also simple and fast.

The quadrupole lenses are assumed to be thin and implemented numerically by applying to each particle impulsive accelerations, Δv_x and Δv_y proportional to the x and y displacement of that particle from the center of the system. v_z is assumed unity for convenience and the particles are then given an impulsive acceleration

$$\begin{aligned} \Delta v_x &= -(x-x_o)\delta \\ \Delta v_y &= (y-y_o)\delta \end{aligned} \tag{7}$$

when passing through a lens which is focussing in the x direction (defocussing in the y direction). Here (x_o, y_o) is the center of the system and $\delta = 1/F$, where F is the focal length of the lens. In the absence of space charge the particles will then coast between lenses according to Eq. (6) so that the numerical system reproduces the thin lens system to within machine roundoff.

Because of the finite grid on which the electric field is defined, space charge phenomena can be resolved only on the scale of a grid cell. Because Poisson's equation is only solved once per time step the charge density can not be allowed to vary significantly within a time step. The physical implications of these statements will be dealt with in the next section.

III. Tests of the Numerical Model

Because the numerical model being employed follows many particles in their self-consistent orbits the large class of nonlinearities possible in an "n-body problem," where n is several thousand, may be present. The details of the physical behavior to be modeled may therefore be quite complex. The numerical system should do a good job of modeling the "important" behavior, where important is defined in terms of the behavior of the average system parameters. For example, if the physical system is unstable to a perturbation whose characteristic wavelength is smaller than a cell size, this behavior may be missed entirely, or at least poorly represented, because of the inability of the numerical system to resolve phenomena on this scale. The same may be true for perturbations with growth times much smaller than a timestep. Lacking a complete theory of the system behavior, such questions must be resolved experimentally by varying the numerical parameters until a regime is found where the system behavior is insensitive to numerical parameters. From similar simulations in plasma physics where particle dynamics are dominated by the collective nature of the electric fields, it may be expected that the time step must be of order the plasma oscillation time

(ω_p^{-1}) and the length scale should be of order a characteristic length defined by the maximum velocity divided by the plasma frequency (analogous to the Debye length).

Preliminary designs for transport systems[1] have assumed a rough balance between magnetic focussing forces and space charge defocussing forces. Accordingly, numerical tests have been run on a transport system which is in this range of parameters.

Magnet strength in the test case has been chosen to correspond to a phase shift per doublet of 90^o as defined in Eq. 1. In the absence of space charge, as in the case which was shown in Fig. 1, it is possible to calculate the initial conditions for a matched system analytically. However, in the presence of space charge, it is most convenient to calculate the initial condition for a matched system iteratively. Successive guesses are obtained by following the system through a doublet lens system, from t=o to $t=2\tau$. The x extent of the next guess is chosen as the average of x extent initially and after one doublet holding the emittance, $x\ p_x$, constant. Similarly, the y extent at $t=2\tau$ is used to calculate a new averaged y dimension. This procedure usually converges in just a few iterations. Fig. 3 shows the initial conditions thus found at the center of a lens which is focussing in the x direction, for a slightly mismatched system with a phase shift per doublet of $\mu_o = \pi/2$. A mismatch of about 10% was chosen so the system would evolve fairly rapidly and thereby test the numerics. Four projections of the density in $x\text{-}p_x\text{-}y\text{-}p_y$ space are shown for 2000 sample particles. The distances labelled on the axes are in terms of program grid points and velocities

are in units of cells/τ. The initial space charge density is such that the Q defined in Eq. 4 is equal to 3.9. In this case the phase shift per doublet is about 30^{o}. The particle positions and momenta are set up using the formulae

$$\begin{aligned} x &= x_o \sqrt{q} \cos\left(\frac{r}{2\pi}\right) \\ p_x &= p_{xo} \sqrt{q} \sin\left(\frac{r}{2\pi}\right) \\ y &= y_o \sqrt{1-q} \cos\left(\frac{s}{2\pi}\right) \\ p_y &= p_{yo} \sqrt{1-q} \sin\left(\frac{s}{2\pi}\right) \end{aligned} \tag{8}$$

where q, r, and s are uniformly distributed random numbers between zero and unity.

The Poisson solver uses Fourier transforms and periodic boundary conditions to solve for the electric field from the particle charge distribution. Since it is impractical to follow the trajectories of as many particles as are actually found in a beam, anomolously high fluctuations in density occur in a particle code simulation. In addition, following only a finite number of modes leads to a band-limited situation in which short wavelength overshoots can occur in the vicinity of sharp changes in charge density. Both these effects can be mitigated somewhat by considering "macro-particles" with a Gaussian charge density.[7] When this is done, the points plotted as in Fig. 3 are really the centers of these "macroparticle" charge clouds rather than point particles.

Fig. 4a is a plot of E_x vs x for a y coordinate 1/2 cell off the center of a 64 x 64 system whose initial conditions are similar to those shown in Fig. 3. Fig. 4b is a plot of the same fields with Gaussian smoothing applied to the system so that the particle "size" between 1/e points on the Gaussian is one cell. Note that E_x is really the average field applied to the smoothed cloud, i.e., the acceleration field. The smoothed fields are closer to linear near the center but the peaks at the edge of the beam are somewhat rounded. Figs. 5 and 6 are a comparison of the phase space of two systems after traversing 16 focussing magnet pairs with and without smoothing. The comparison time was chosen because of the fine structure at this time which ought to accentuate numerical differences. Figs. 5 and 6 are phase space plots which correspond to the same smoothing as in Figs. 4a and 4b respectively. Though there are minor differences, they do not appear to be significant and they are small compared with differences which arise from changing the number of grid cells and which will be dealt with later. In both Figs. 5 and 6, 2048 particles are shown out of the 4096 used in the run. Other parameters are $\Delta t = .2\tau$, 64 x 64 cells and $\omega_p \tau = 1.2$. Since the smoothing does not have a major effect on the short time system evolution and does not seem to negatively affect evolution of the beam edge, there is a net advantage to employing it for long times in order to avoid anomolous fluctuation effects.

In simulating a collisionless plasma, it is usually impractical to represent anything like the number of particles in a real system. Consequently the number of particles per Debye volume is low. The simulation may then represent the collisionless behavior only for a number of

plasma periods proportional to the reciprocal of the actual number of simulation particles in a Debye volume. Fig. 7 is a phase space plot from a calculation with conditions as in Fig. 6 but with double the number (8192) of simulation particles. While the fine structure changes slightly, mainly in the y-P_y view, the computed results are essentially independent of the number of simulation particles; the small residual differences are due as much to different statistics in the initial distribution as to fluctuations in the fields during the run. The difference is made more noticeable in Fig. 8 by again doubling the number of particles to 16384. Here, too, however, it is felt that any differences are due to different statistics.

The Fourier Transform Poisson solver employed uses periodic boundary conditions. This means that the neutralizing charges, instead of being at infinity or in finite images are, uniformly distributed throughout the system. Furthermore each beam particle has an image of the same sign and size one system length away in each direction. Such a computational system clearly reproduces the infinite system when the boundary is far enough away.

Fig. 9 shows results from a calculation using a 128 by 128 finite difference mesh where the beam occupies only one quarter of the system area of the previous runs. That is, measured in beam size, the boundaries are twice as far out as in the previous runs. The numerics are otherwise identical to Fig. 6. The behavior of the two systems is again quite similar, showing that the boundary conditions are not having a major effect.

We have thus far seen that, when run through 16 magnet pairs, the system behavior is relatively insensitive to varying the particle smoothing, the number of particles and the distance to the boundaries.

A comparison of Fig. 6 with Fig. 10 shows the differences in behavior caused by changes in the resolution. Fig. 6 uses twice as many cells in the description of the electric fields of the beam and fine structure has appeared which was not present in the coarser grid run of Fig. 10. A comparison of Figs. 9 and 11 shows the result of doubling the resolution again. Fig. 9 is a 64 x 64 system and Fig. 11 is 128 x 128. Each run has 16K particles. (The number of sample particles for plotting is still 2K.) Though the difference is not as great as the original doubling, more fine structure is evident.

Finally, Fig. 12 shows the effect of taking twice as many timesteps (20) per magnet period. The parameters are otherwise the same as the run in Fig. 11. A comparison of the two pictures shows that the two are extremely close.

It is evident from these series of tests that the numerics are indeed capable of affecting the fine structure of the phase space distribution of the beam particles. The important question is whether differences in the fine structure have any important physical significance. Though the question can only be answered definitively when the physics of space charge effects in particle transport systems is well understood, there are several reasons for confidence that the numerical results will be reliable.

The fine structure observed in these runs is probably a consequence of the sharp edge of the distribution function. This particular initial distribution was chosen because the K-V distribution is well understood theoretically. It is not a physically realistic distribution because of the very sharp edges. A more physical distribution would have diffuse edges and the fine structured behavior would then be washed out. Some evidence has already been obtained that this is the case. In fact, it appears as if a steady state can be reached which is independent of the numerical parameters and the details of the intermediate turbulent structure.

That the numerical system can do as good a job as it does in examining the behavior of the sharp edged K-V distribution is encouraging since this type of system is generally the most difficult one to treat *numerically*. It seems clear that the similarities in behavior over a large range of numerical parameters indicate that reliable data on focussed beam systems can be inferred from this approach. Furthermore, because of the flexibility of this numerical approach it is easily possible to include many complexities such as finite length lenses and lens non-linearities which can give valuable insight into design of practical transport systems. Initial simulations to gain insight into the physics of beam transport systems in the presence of space charge should concentrate on simple systems and these are currently underway.

Acknowledgment

The author wishes to acknowledge the assistance and encouragement provided by Drs. J. P. Boris, T. F. Godlove, L. J. Laslett, A. W. Maschke, and L. Smith.

References

1. Final Report of ERDA Summer Study of Heavy Ions for Inertial Fusion, LBL-5543 (Dec. 1976).

2. "Focussing of Charged Particles," Edited by Albert Septier, Academic Press, New York (1967).

3. I.M. Kapchinsky and V.V. Vladiminsky, Proc. Internat. Conf. on High Energy Accelerators, CERN 1959, p. 274.

4. G. Lambertson, L.J. Laslett and L. Smith, IEEE Transactions on Nuclear Sci., NS-24, p. 993. Jun 1977

5. T.K. Khoe and R.L. Martin, IEEE Transactions on Nuclear Sci., NS-24, p. 1025. Jun 1977

6. Methods in Computational Physics, Vol. 9, "Plasma Physics," Academic Press, New York (1970); Methods in Computational Physics, Vol. 16, "Controlled Fusion," Academic Press, New York (1976).

7. Methods in Computational Physics, Vol. 9; op. cit., p.1.

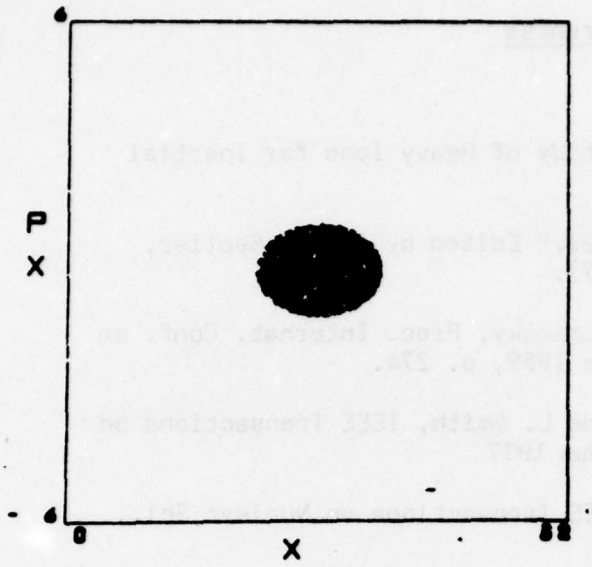

(a)

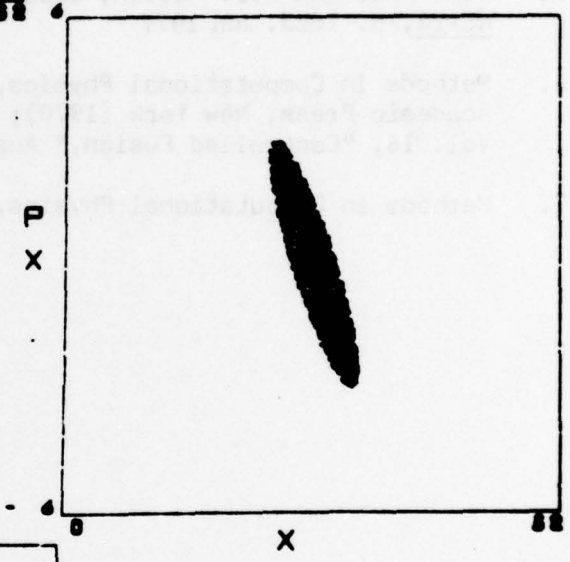

(b)

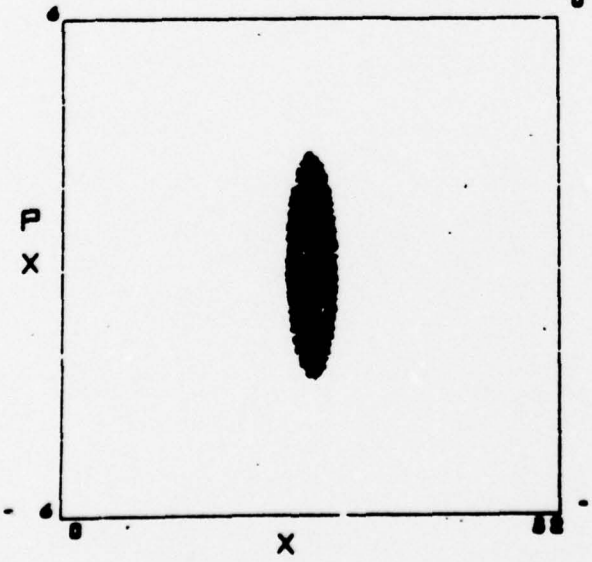

(c)

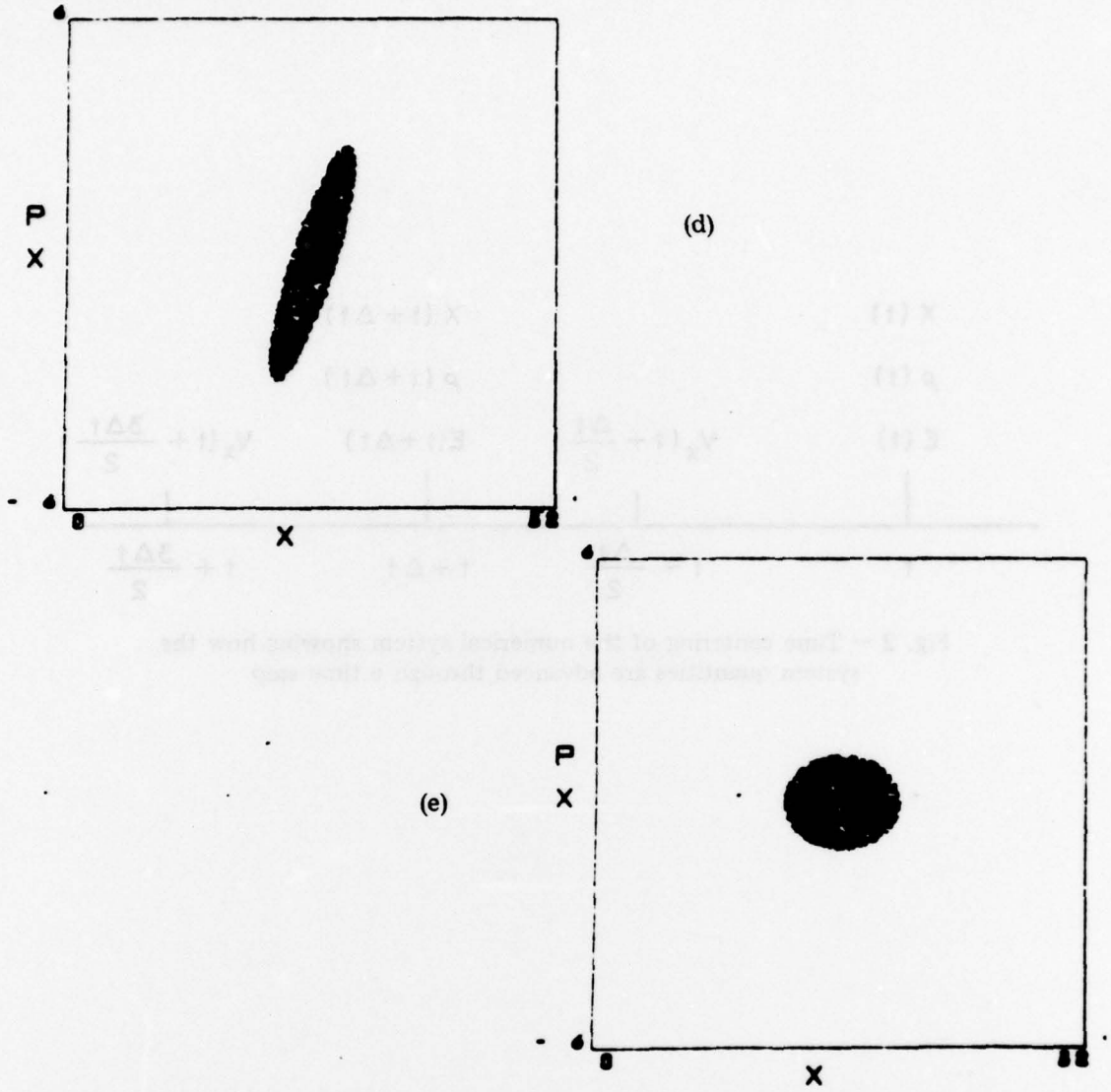

Fig. 1 — x-p_x phase space plot showing the evolution of a matched phase space ellipse of particles as it passes through a lens system with a phase shift of 90° per doublet. Fig. 1a shows the initial distribution halfway through a focussing lens. Fig. 1b shows the distribution 2/5 of the distance to the next lens. Fig. 1c shows the distribution halfway through a defocussing lens. Fig. 1d is 4/5 through the doublet. Finally, Fig. 1e is one complete lens period away showing a return to the initial elliptical shape.

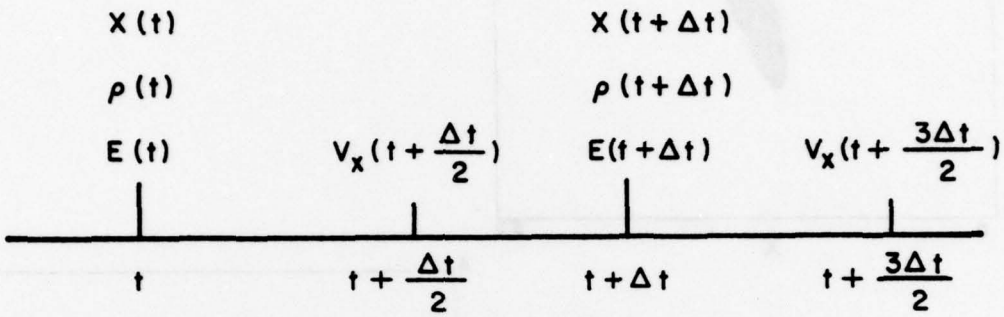

Fig. 2 — Time centering of the numerical system showing how the system quantities are advanced through a time step

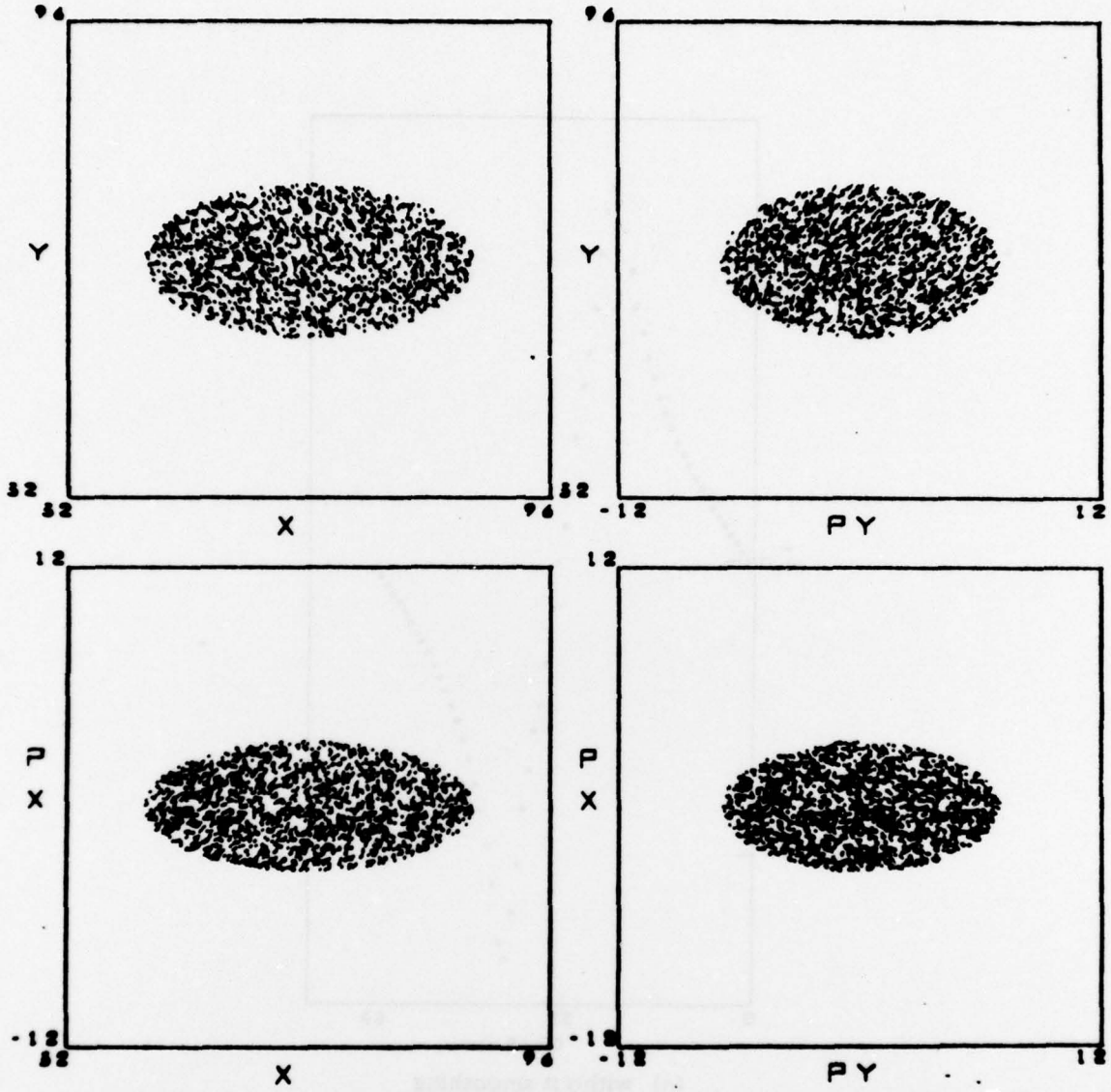

Fig. 3 — Initial phase space ellipses of a slightly mismatched Kapchinskij-Vladimirkij distribution with a magnet tune of 90° per doublet and enough space charge to bring the tune down to 30°. Units of length are in cells and units of velocity are in cells/τ where τ is the time between successive magnets. Center of the beam is the center of the numerical system so that the system size (128 x 128) can be inferred from the labels on the configuration space axes. 2048 sample particles are plotted.

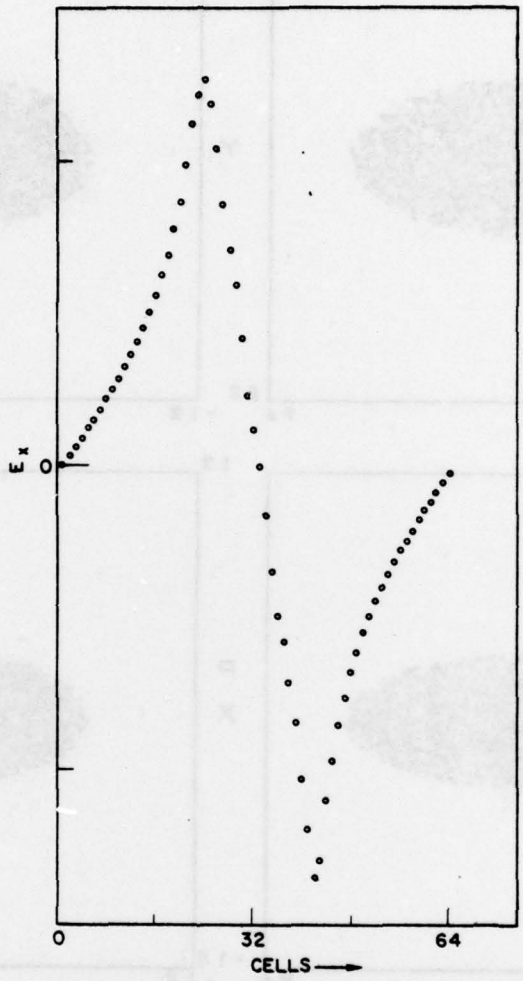

(a) without smoothing

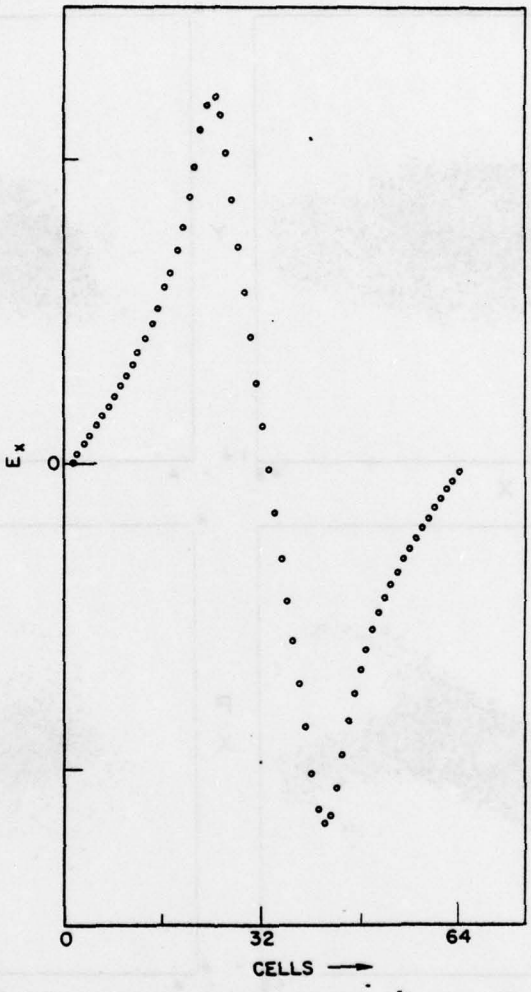

(b) with a particle 1/e width of one cell

Fig. 4 — Near axis force field in a 64 x 64 system with and without smoothing

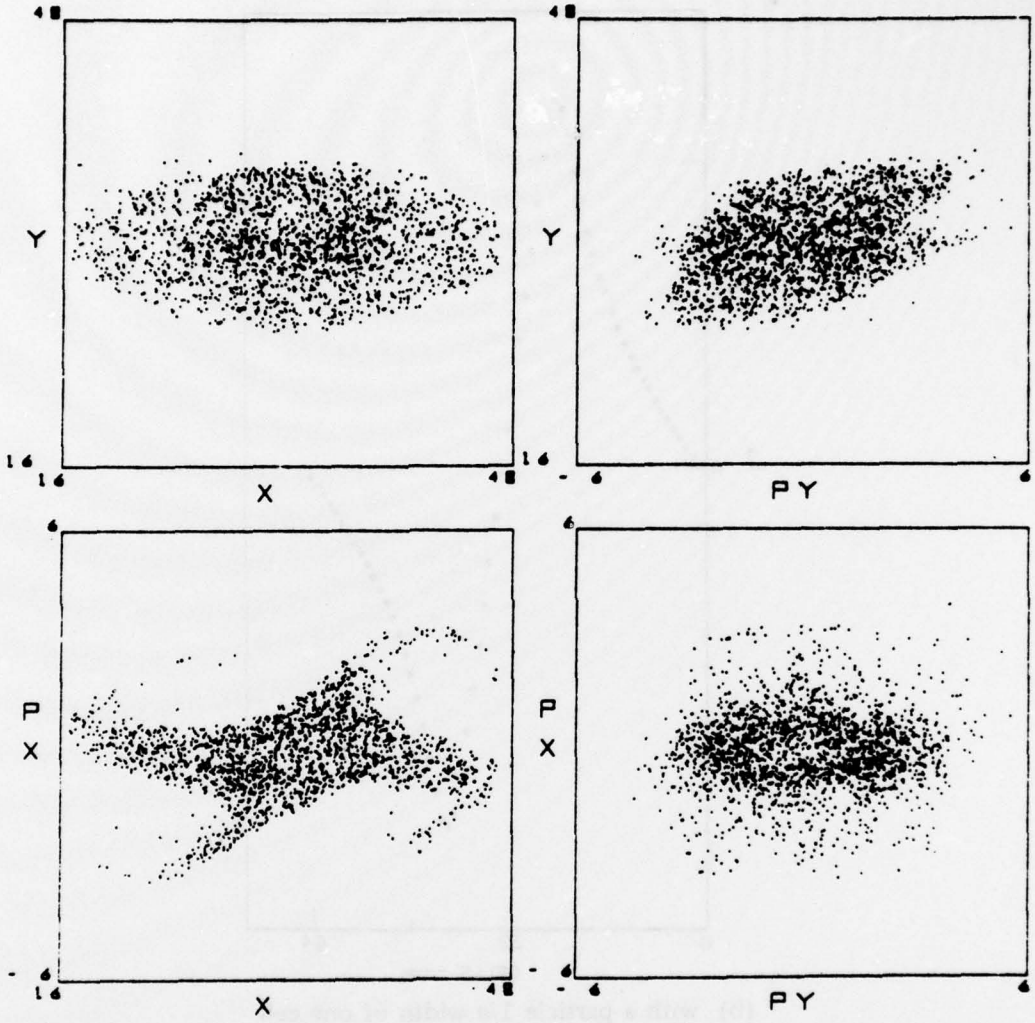

Fig. 5 — Phase space of a 64 x 64 system showing 2048 sample particles of 4096 in the system after 16 magnet pairs of 160 time steps. (τ = 32) No smoothing was used.

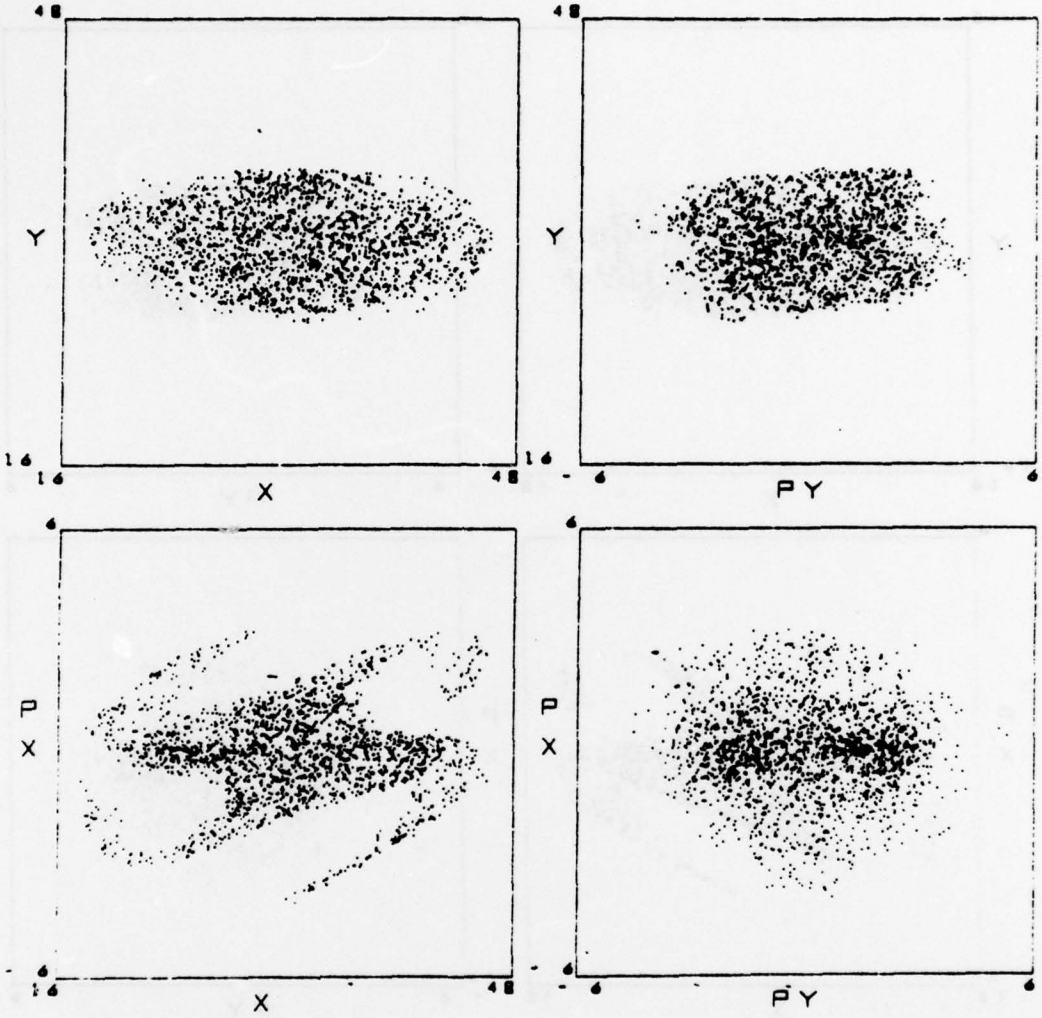

Fig. 6 — Phase space of a 64 x 64 system with a 1/e width of one cell

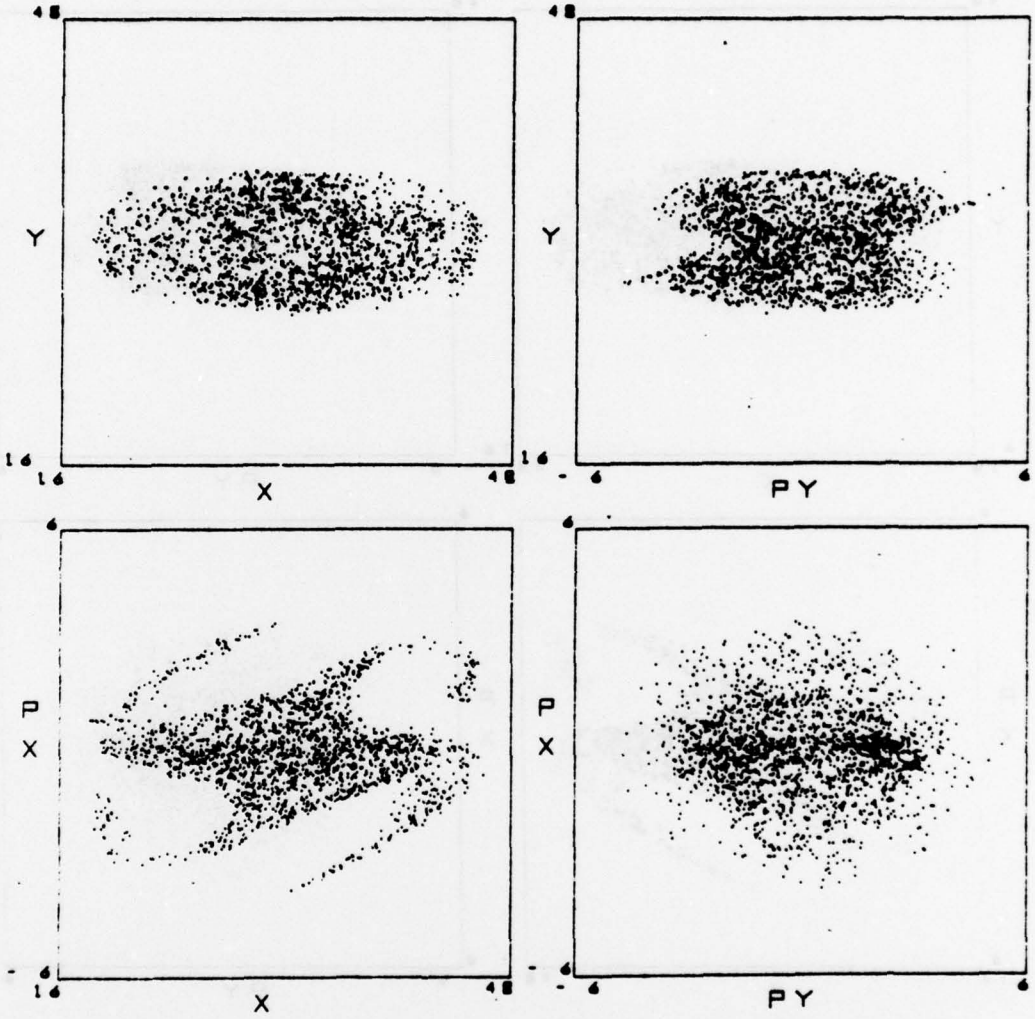

Fig. 7 — Phase space of a 64 x 64 system as in Fig. 4 again showing 2048 sample particles but with twice as many particles (8192) in the system

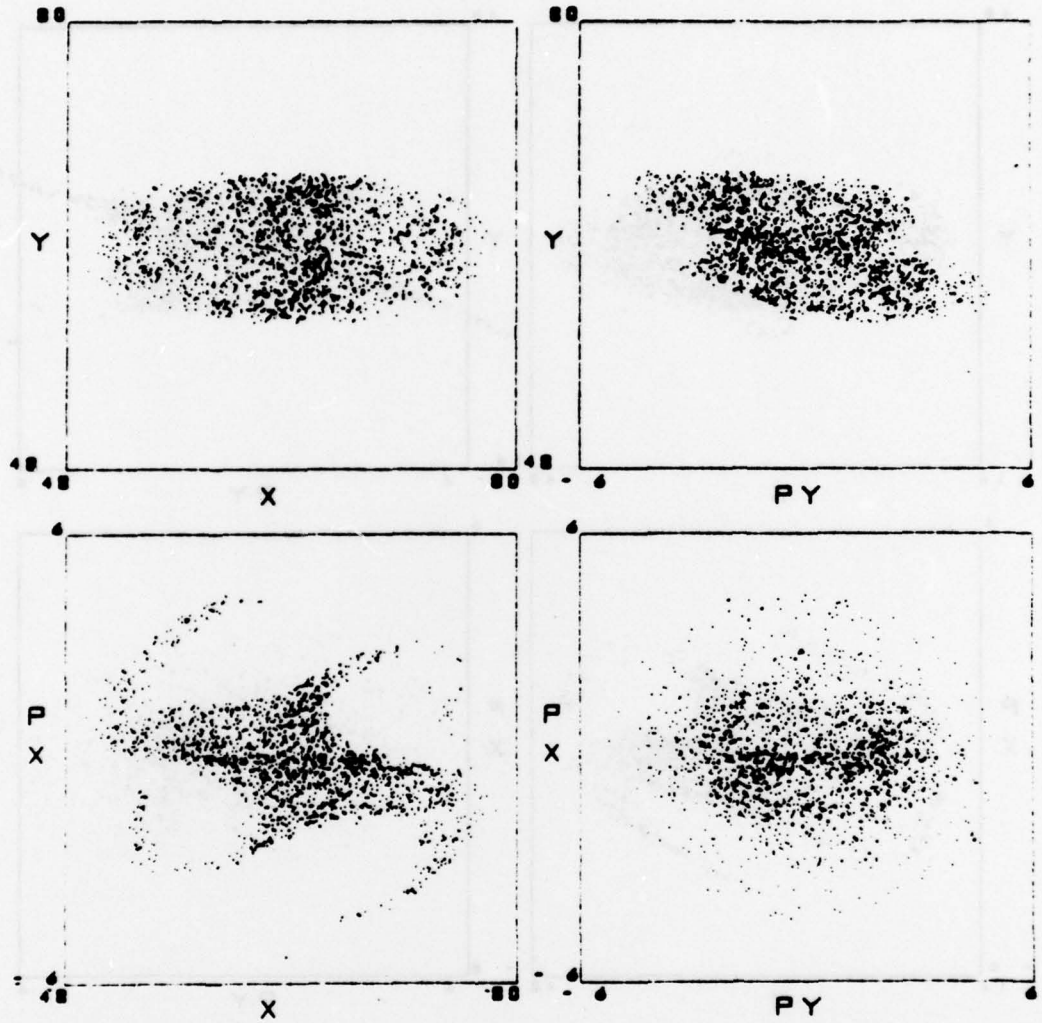

Fig. 8 — Phase space of a 64 x 64 system with the number of particles again doubled (to 16284)

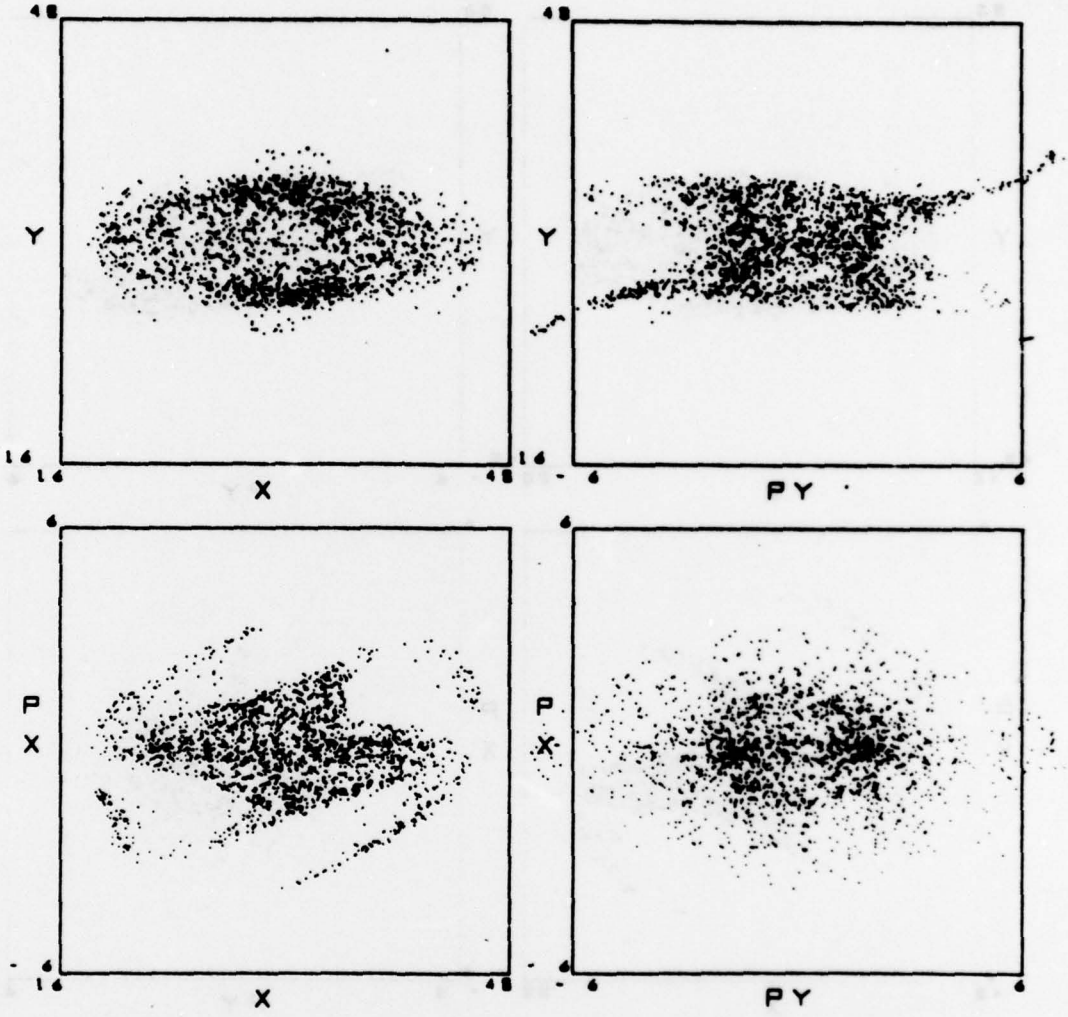

Fig. 9 — Phase space of a 128 x 128 system with 4096 particles. The resolution describing the beam is unchanged but the boundaries are twice as far away.

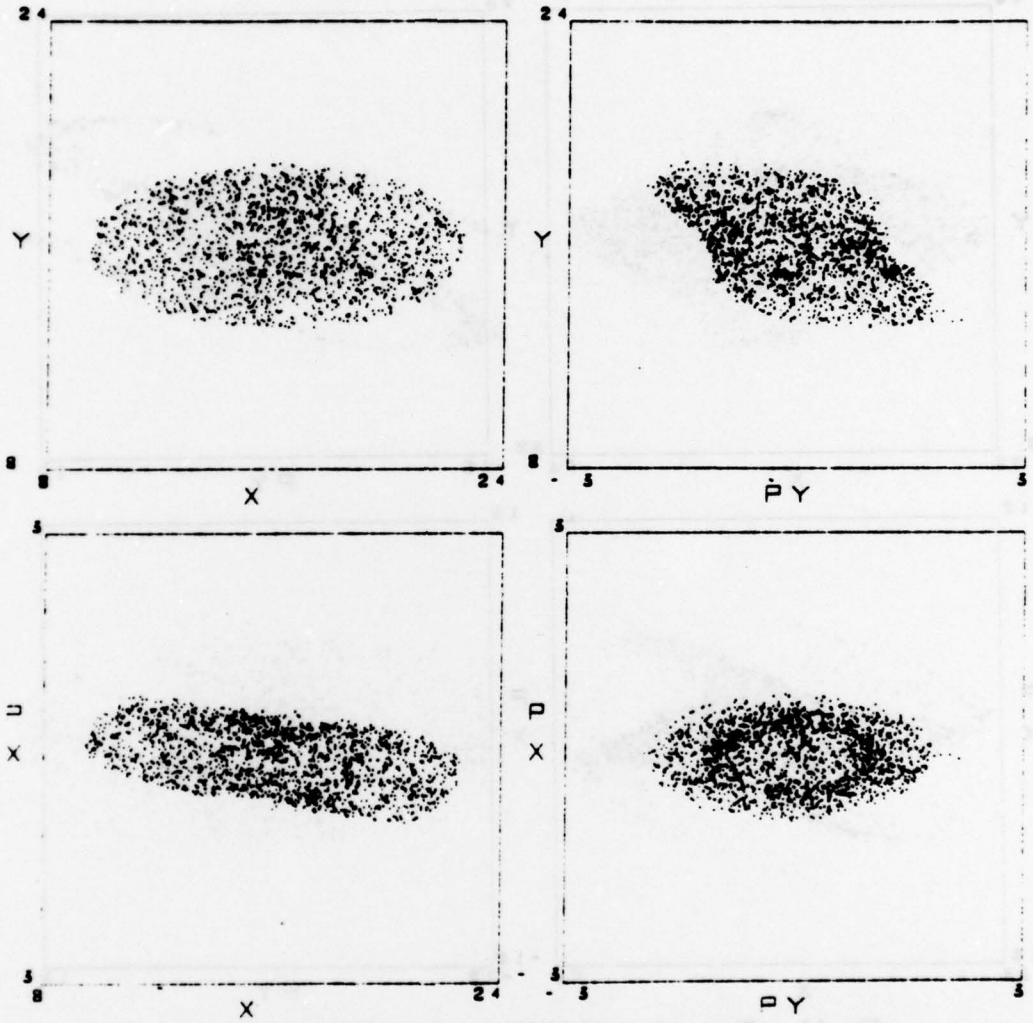

Fig. 10 — Phase space of a 32 x 32 system illustrating the effect of a coarser resolution of the fields

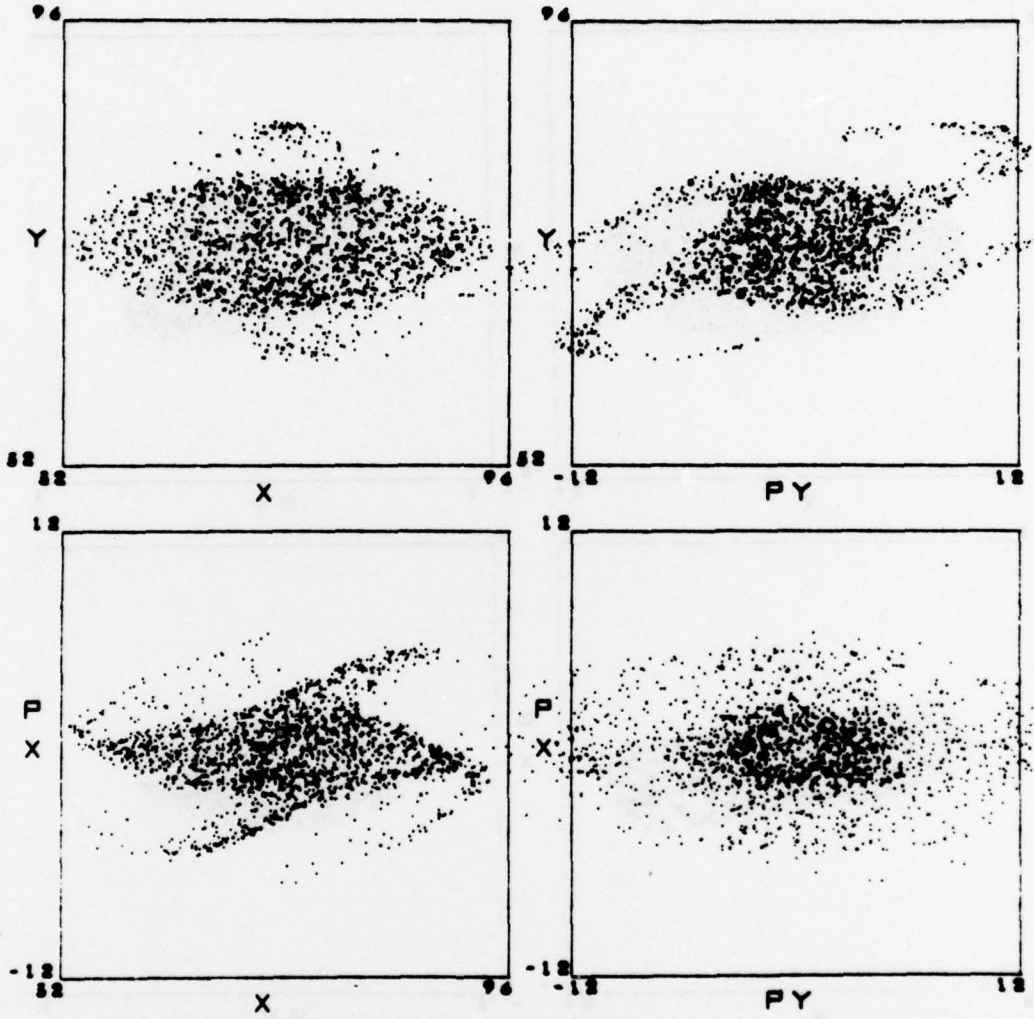

Fig. 11 — Phase space of 2048 sample particles on a system with sixteen thousand particles and 128 x 128 grid points showing the effect of the greater resolution on the fine structure of the system evolution

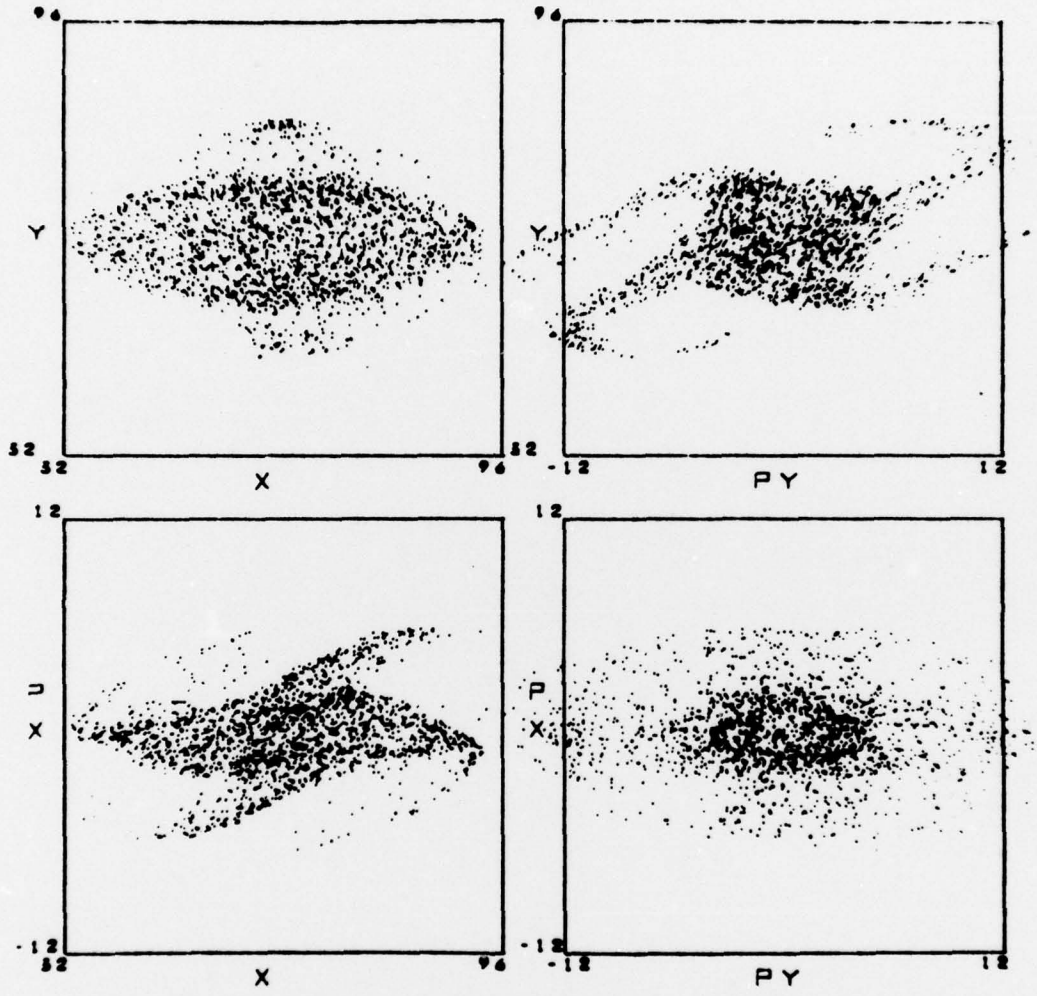

Fig. 12 — Phase space of a 128 x 128 system with 16384 particles and 20 timesteps per magnet pair

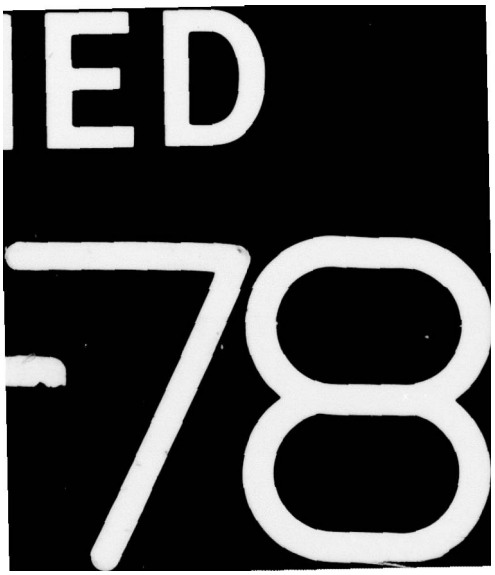
ED
78